International Journal of Thermophysics, Vol. 22, No. 2, 2001

Thermodynamic Property Model for Fluid-Phase *n*-Butane[1]

H. Miyamoto[2, 3] and K. Watanabe[2]

A Helmholtz free energy equation of state for the fluid phase of *n*-butane (R-600) has been developed on the basis of the ITS-90 temperature scale. This model has been established on the basis of selected measurements of the pressure–density–temperature (P, ρ, T), isochoric heat capacity, speed of sound, and the saturation properties. The linear structural regression optimization and nonlinear fitting procedure were used to determine the functional form and the numerical parameters of the present equation of state. Based on a comparison with available experimental data, it is recognized that the developed model represents most of the reliable experimental data accurately in the range of validity covering temperatures from 134.87 K (the triple-point temperature) to 589 K, at pressures up to 69 MPa, and at densities up to 745 $kg \cdot m^{-3}$. The reasonable behaviors of the derived thermodynamic properties have also been confirmed over the entire fluid phase of *n*-butane.

KEY WORDS: equation of state; Helmholtz free energy; hydrocarbon; natural working fluid; *n*-butane; R-600; refrigerant; thermodynamic property.

1. INTRODUCTION

Hydrocarbon (HC) refrigerants are recognized as components of several promising alternative mixtures for refrigeration and air-conditioning systems because of their zero ODP and negligible GWP values. By blending them with nonflammable hydrofluorocarbon (HFC) refrigerants, the flammability of HCs and larger GWP values of HFCs can be simultaneously reduced. If the flammability issue can be resolved in advanced refrigeration-based

[1] Paper presented at the Fourteenth Symposium on Thermophysical Properties, June 25–30, 2000, Boulder, Colorado, U.S.A.

[2] Department of System Design Engineering, Faculty of Science and Technology, Keio University, 3-14-1, Hiyoshi, Kohoku-ku, Yokohama 223-8522, Japan.

[3] To whom correspondence should be addressed. E-mail: miya@ws.sd.keio.ac.jp

0195-928X/01/0300-0459$19.50/0

systems, HC refrigerants including propane (R-290), *n*-butane (R-600), isobutane (R-600a), and their mixtures may also become promising.

Taking such a background into account, accurate equations of state for pure HCs and pure HFCs are needed for development of thermodynamic property models of their mixtures. Accurate equations of state for pure HFCs have recently become available, including fundamental equations of state formulated in terms of a nondimensional Helmholtz free energy for R-32, R-134a, and R-143a by Tillner-Roth and Yokozeki [1], Tillner-Roth and Baehr [2], and Lemmon and Jacobsen [3], respectively, all of which were accepted as international standard equations of state by the IEA (International Energy Agency)—Annex XVIII. Regarding the HCs, a Helmholtz free energy model has been developed for propane by the present authors [4] on the basis of available experimental data. As a continuation, in the present study, we have formulated an accurate Helmholtz-type model for the fluid phase of *n*-butane.

Among the available thermodynamic property models for *n*-butane, the model by Younglove and Ely [5] has been widely used in various applications including REFPROP (Version 6.01) [6]. However, it was developed based upon available experimental data by the mid-1980s and the IPTS-68 temperature scale. Recently, several new measurements on $P\rho T$, caloric, and acoustic properties for *n*-butane became available, and therefore, we have developed a new model on the basis of these new experimental data and the new ITS-90 temperature scale, to serve as the basis for development of thermodynamic property models for HFC mixtures with *n*-butane.

2. SELECTION OF INPUT DATA

We collected about 2000 experimental thermodynamic property measurements for *n*-butane. A summary of data in the single-phase region, such as $P\rho T$, caloric, and acoustic property measurements, and saturation property data, including vapor pressures, saturated vapor and liquid densities, liquid heat capacities, and speeds of sound, is listed in Table I. Most of the experimental thermodynamic property data reported prior to 1982 were summarized by Haynes and Goodwin [28]. For our model, the temperature values of all experimental data are converted to ITS-90, except for a set of $P\rho T$ property data in the vapor phase by Gupta and Eubank [11], isochoric heat capacities in the liquid phase by Magee and Lüddecke [12], and a set of saturated-liquid heat capacities by Magee and Lüddecke [12], all of which have been published recently.

In the single-phase region, three sets of experimental $P\rho T$ property data (Fig. 1), by Olds et al. [9], Haynes [10], and Gupta and Eubank [11], which are indicated with asterisks in Table I, were used as input

data. Other sets of $P\rho T$ data were used only to compare with the developed formulation; these include the data of Beattie et al. [7] and a set of data by Kay [8] that includes a large quantity of calculated values extrapolated from the original measurements by the author. Regarding caloric and acoustic properties (Fig. 2), three sets of experimental measurements, a set of isochoric heat capacity, C_V, data of Magee and Lüddecke [12] and two sets of speed-of-sound, W, data of Niepmann [15] and Ewing et al. [16], were also used as input data. The experimental isobaric heat capacity, C_P, data of Sage et al. [13] were not used as input data.

The saturation property data used for our model are also indicated with asterisks in Table I. Regarding the saturated vapor pressures, P_S, saturated vapor and liquid densities, ρ'' and ρ', these selected data were used to provide three sets of supplementary input data calculated from the ancillary correlations discussed in the next section. The saturated-liquid heat capacity, C_σ, data of Magee and Lüddecke [12] and saturated-liquid speed-of-sound, W', data of Niepmann [15] were directly used as additional input data only in the nonlinear fitting process.

3. ANCILLARY CORRELATIONS

In the present study, the following three ancillary correlations for P_S, ρ'', and ρ' were developed on the basis of the selected experimental data indicated with asterisks in Table I.

$$\ln \frac{P_S}{P_C} = \frac{1}{1-x}\left(A_1 x + A_2 x^{1.5} + A_3 x^{2.0} + A_4 x^{4.5}\right) \tag{1}$$

$$\ln \frac{\rho''}{\rho_C} = B_1 x^{0.33} + B_2 x^{0.9} + B_3 x^{2.4} + B_4 x^{4.9} + B_5 x^{10} \tag{2}$$

$$\ln \frac{\rho'}{\rho_C} = C_1 x^{0.3} + C_2 x^{1.3} + C_3 x^{1.7} \tag{3}$$

Equations (1), (2), and (3) correspond to the saturated vapor pressure, saturated vapor density, and saturated liquid density, respectively. In each correlation, $x = 1 - T/T_C$, where T_C denotes the critical temperature, 425.125 K, P_C is the critical pressure, 3.796 MPa, and ρ_C is the critical density, 227.84 $kg \cdot m^{-3}$, as discussed in the next section, and the coefficients are listed in Table II. In our development of these correlations, we used a set of P_S values determined by Magee [29] and a set of ρ'' values calculated from Eq. (1) with a truncated virial equation of state with the

Table I. Sources of Experimental Thermodynamic Property Data for Normal Butane

				P		ρ		T	
First author[a]	Ref.	Property	No. of data	Range (MPa)	δP^b (%)	Range ($kg \cdot m^{-3}$)	$\delta\rho$ ($kg \cdot m^{-3}$)	Range (K)	δT^b (mK)
Beattie	[7]	$P\rho T$	116	1.5–36	n.a.	29–494	n.a.	423–573	n.a.
Kay	[8]	$P\rho T$	453	0.2–8.3	0.4	4.6–513	0.15%	311–589	60
Olds*	[9]	$P\rho T$	217	0.1–69	0.1	0.9–632	0.10%	311–511	6
Haynes*	[10]	$P\rho T$	105	1.7–36	0.01	572–745	0.10%	140–300	10 (30)
Gupta*	[11]	$P\rho T$	49	0.0–1.1	n.a.	0.4–19	n.a.	265–450	n.a.
Magee*	[12]	C_V	148	1.9–33	n.a.	546–720	0.20%	153–342	n.a.
Sage	[13]	C_P	8	0.1	0.1			294–411	60
Dailey	[14]	C_P	8	0.1	n.a.			345–693	n.a.
Niepmann*	[15]	W	230	0.1–60	n.a.			200–375	n.a.
Ewing*	[16]	W	78	0.0–0.1	n.a.			250–320	n.a.
Kay	[8]	P_S	20	0.5–3.8	0.4			325–425	60
Kahre	[17]	P_S	2	0.2–0.5	n.a.			289–328	n.a.

Flebbe*	[18]	P_S	12	0.1–1.1	0.015 (100 Pa)			278–358	7
Kratzke*	[19]	P_S	12	0.5–3.7	0.03			320–423	10
Holldorff	[20]	P_S	20	0.1–1.1	0.1			259–357	40
Machin	[21]	P_S	224	0.0–0.1	0.06 (0.3 Pa)			173–280	2
Sako	[22]	P_S	22	0.3–0.4	0.3 kPa			301–316	30
Kay	[8]	ρ''	20			13–228	0.15%	325–425	60
Olds*	[9]	ρ''	4			8.9–97	0.10%	311–411	6
Sliwinski*	[23]	ρ''	10			4.0–35	0.05	283–368	n.a.
Kay	[8]	ρ'	20			228–541	0.15%	325–425	60
Olds	[9]	ρ'	4			372–557	0.10%	311–411	6
Sliwinski*	[23]	ρ'	10			476–590	0.05	283–368	n.a.
McClune*	[24]	ρ'	7			700–727	0.10%	143–173	100
Haynes*	[25]	ρ'	12			570–735	0.10%	135–300	40
Orrit*	[26]	ρ'	50			598–735	0.4	135–275	n.a.
Aston	[27]	C_σ	21					140–268	n.a.
Magee*	[12]	C_σ	100					139–317	n.a.
Niepmann*	[15]	W'	19	0.0–1.2	n.a.			200–360	n.a.

[a] Data used as input data are denoted by a superscript asterisk.
[b] Figures in parentheses denote the maximum experimental uncertainty claimed.

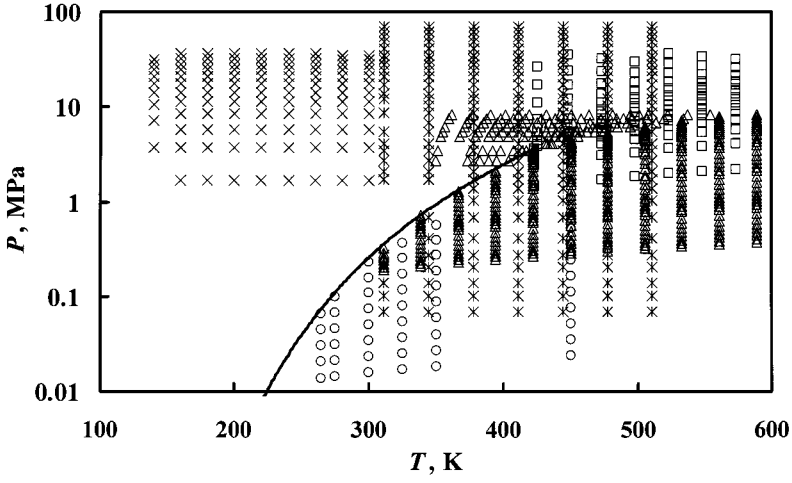

Fig. 1. Distribution of experimental $P\rho T$ property data. (□) Beattie et al. [7]; (△) Kay [8]; (∗) Olds et al. [9]; (×) Haynes [10]; (○) Gupta and Eubank [11].

same functional form that we used for propane [4]. It was developed based on the available $P\rho T$ property data in the vapor phase of *n*-butane below the critical temperature so as to generate additional ρ'' values at temperatures below 280 K, where no measurements exist. It is noted that these two sets of calculated values were also used to cover the range of temperatures

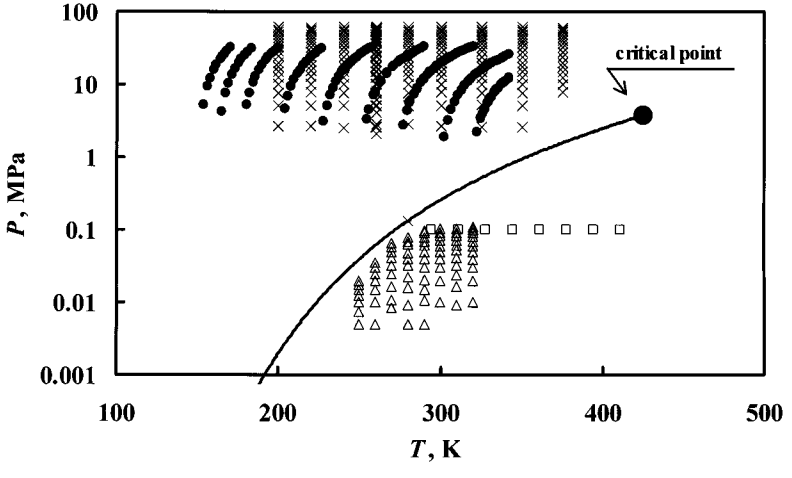

Fig. 2. Distribution of caloric and acoustic property data. (□) [C_P] Sage et al. [13]; (×) [W] Niepmann [15]; (△) [W] Ewing et al. [16]; (●) [C_V] Magee and Lüddecke [12].

Table II. Coefficients of Eqs. (1)–(3)

i	A_i	B_i	C_i
1	−7.246998	−1.903334	1.378063
2	2.899084	−4.860578	−0.4003577
3	−2.506508	−11.11094	0.3561708
4	−2.460527	−28.93348	
5		−73.96275	

below 280 K, and therefore, Eqs. (1)–(3) are valid for temperatures from the triple point to the critical point.

4. FUNDAMENTAL EQUATION OF STATE

The dimensionless Helmholtz free energy, $\phi(\tau, \delta)$, model is given by Eq. (4), where the ideal-gas state contribution, $\phi^0(\tau, \delta)$, is expressed by Eq. (5) and the residual real-fluid contribution, $\phi^r(\tau, \delta)$, by Eq. (6). Independent variables are the inverse reduced temperature, $\tau = T_C/T$, and the reduced density, $\delta = \rho/\rho_C$, while f denotes the Helmholtz free energy.

$$\phi(\tau, \delta) = \frac{f}{RT} = \phi^0(\tau, \delta) + \phi^r(\tau, \delta) \tag{4}$$

$$\phi^0(\tau, \delta) = \ln \delta + a_1^0 + a_2^0 \tau + a_3^0 \ln \tau + \sum_{i=4}^{7} a_i^0 \ln[1 - \exp(-n_i \tau)] \tag{5}$$

$$\phi^r(\tau, \delta) = \sum_{i=1}^{8} a_i \tau^{t_i} \delta^{d_i} + \sum_{i=9}^{13} a_i \tau^{t_i} \delta^{d_i} \exp(-\delta) + \sum_{i=14}^{16} a_i \tau^{t_i} \delta^{d_i} \exp(-\delta^2) + \sum_{i=17}^{19} a_i \tau^{t_i} \delta^{d_i} \exp(-\delta^3) \tag{6}$$

In the present model, $T_C = 425.125$ K, $\rho_C = 227.84\ \text{kg} \cdot \text{m}^{-3}$, and $P_C = 3.796$ MPa, determined by Haynes and Goodwin [28], are used as reducing parameters, and R is the gas constant for *n*-butane with $R = R_m/M$, where the universal gas constant, $R_m = 8.314472\ \text{J} \cdot \text{mol}^{-1} \cdot \text{K}^{-1}$ [30], and the molar mass, $M = 58.1222\ \text{g} \cdot \text{mol}^{-1}$ [31], are adopted.

The coefficients of $\phi^0(\tau, \delta)$ are listed in Table III. In Eq. (5), the first term of $\ln \delta$ is related to the ideal-gas law, and the coefficients a_1^0 and a_2^0 are determined in accord with the reference values of specific enthalpy and

Table III. Coefficients of Eq. (5)

i	a_i^0	n_i
1	−5.404217	—
2	4.911360	—
3	3.240207	—
4	5.513671	0.7705025
5	7.38845	3.10278
6	10.25063	9.735094
7	11.06101	4.385458

specific entropy for the saturated liquid at $T_0 = 273.15$ K, i.e., $h'(T_0) = 200$ kJ · kg^{-1} and $s'(T_0) = 1.0$ kJ · kg^{-1} · K^{-1}. The ideal-gas heat capacity, C_P^0, values determined by Chen et al. [32] are reproduced within ±0.05% by Eq. (5) for temperatures from 50 to 1500 K.

The values of the coefficients of the residual real-fluid contribution, $\phi^r(\tau, \delta)$, are also listed in Table IV. To determine the formulation of $\phi^r(\tau, \delta)$, we have used the programs of Tillner-Roth [33], which contain two algorithms: (a) Wagner's linear stepwise regression analysis [34] for determining the structure including the combination of terms by using only the

Table IV. Coefficients and Exponents of Eq. (6)

i	a_i	t_i	d_i
1	2.952054×10^{-1}	−0.25	1
2	-1.326360×10^{0}	1.50	1
3	-2.031317×10^{-3}	−0.75	2
4	2.240301×10^{-1}	0.00	2
5	-3.635425×10^{-2}	1.25	3
6	1.905841×10^{-3}	1.50	5
7	7.409154×10^{-5}	0.50	8
8	-1.401175×10^{-6}	2.50	8
9	-2.492172×10^{0}	1.50	3
10	2.386920×10^{0}	1.75	3
11	1.424009×10^{-3}	−0.25	8
12	-9.393388×10^{-3}	3.00	5
13	2.616590×10^{-3}	3.00	6
14	-1.977323×10^{-1}	4.00	1
15	-3.809534×10^{-2}	2.00	5
16	1.523948×10^{-3}	−1.00	7
17	-2.391345×10^{-2}	2.00	2
18	-9.535229×10^{-3}	19.00	3
19	3.928384×10^{-5}	5.00	15

experimental thermodynamic property data which are linearly related to the Helmholtz free energy and (b) the nonlinear fitting process for adjusting the coefficients, a_i, to the data for any thermodynamic properties simultaneously. Note also that the applicability of the functional form of the present model to other hydrocarbons including propane and isobutane was examined frequently in this procedure. The present model is developed on the basis of ITS-90, and the range of validity of Eq. (4) covers temperatures from 134.87 K (triple point) to 589 K, at pressures up to 69 MPa, and at densities up to 745 $kg \cdot m^{-3}$.

5. COMPARISON WITH EXPERIMENTAL DATA

Pressure deviations of available $P\rho T$ property measurements in the vapor phase from the present model are shown in Fig. 3, while density deviations in the liquid phase are given in Fig. 4. For the vapor phase, the measurements by Gupta and Eubank [11] are well represented within $\pm 0.21\%$ in pressure, whereas the data of Olds et al. [9] agree with Eq. (4) within $\pm 0.44\%$ in pressure except for a single datum, as shown in Fig. 3. The $P\rho T$ data of Beattie et al. [7] and Kay [8], which were not used as input data, are represented within $\pm 0.88\%$ in pressure. Although the maximum deviations of these unused data given here are off-scale from Fig. 3, the absolute average deviation (AAD) with respect to each data set is less than 0.37%. In the liquid phase, the accurate $P\rho T$ data of Haynes [10] are represented within $\pm 0.23\%$ in density, while the data of Olds et al. [9] agree with Eq. (4) within $\pm 0.8\%$ in density except for one data point, as shown in Fig. 4. The unused $P\rho T$ data of Beattie et al. [7] and Kay [8] are represented within $\pm 1.49\%$ in density, where the AAD value of each set of data is 0.83 and 0.36%, respectively.

Figures 5 to 8 show the relative deviations of experimental C_V and W data from Eq. (4). It is clear from these four figures that most of those available measurements for caloric and acoustic properties of *n*-butane are satisfactorily represented within $\pm 2.0\%$ over the effective range of the present model. In the vapor phase, the W data of Ewing et al. [16] are well represented within $\pm 0.11\%$ as shown in Fig. 5. The C_P data in the vapor phase of Sage et al. [13] are found to be obsolete because of the strong systematic deviations, up to -9.2%, from the present model and are not shown in these figures. In the liquid phase, as shown in Figs. 6 and 7, the C_V data of Magee and Lüddecke [12] agree with the present model within $\pm 1.2\%$ except for six data points at lower temperatures below 168 K, whereas the W data of Niepmann [15] are represented within $\pm 1.5\%$. Along the saturation boundary, the C_σ data of Magee and Lüddecke [12] are reasonably represented within $\pm 0.53\%$ at temperatures from 139 to

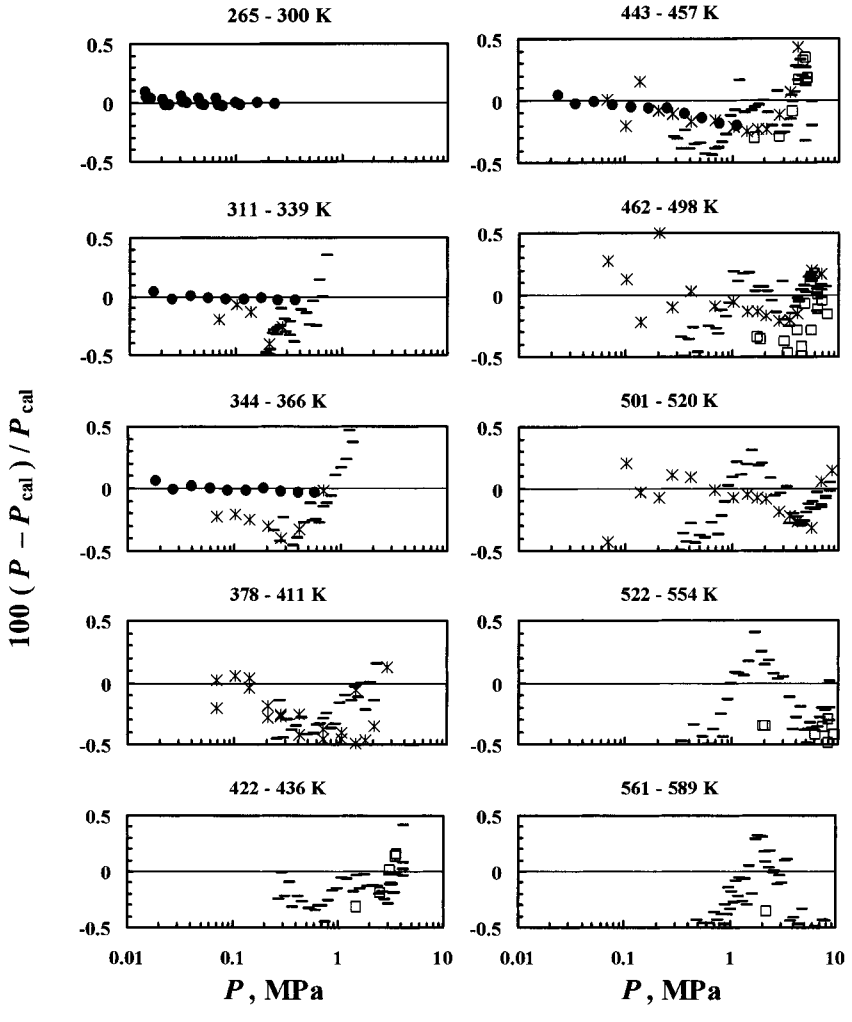

Fig. 3. Pressure deviations of $P\rho T$ property data from Eq. (4). (□) Beattie et al. [7]; (–) Kay [8]; (∗) Olds et al. [9]; (●) Gupta and Eubank [11].

317 K, whereas the W' data of Niepmann [15] are represented within $\pm 0.86\%$, as shown in Fig. 8.

Comparisons of thermodynamic properties along the saturation boundary with the present model are shown in Figs. 9 to 11, in which the behaviors of the calculated values from the modified BWR equation of state developed by Younglove and Ely [5] are also included. The calculated values from three ancillary correlations for P_S, ρ'', and ρ' given

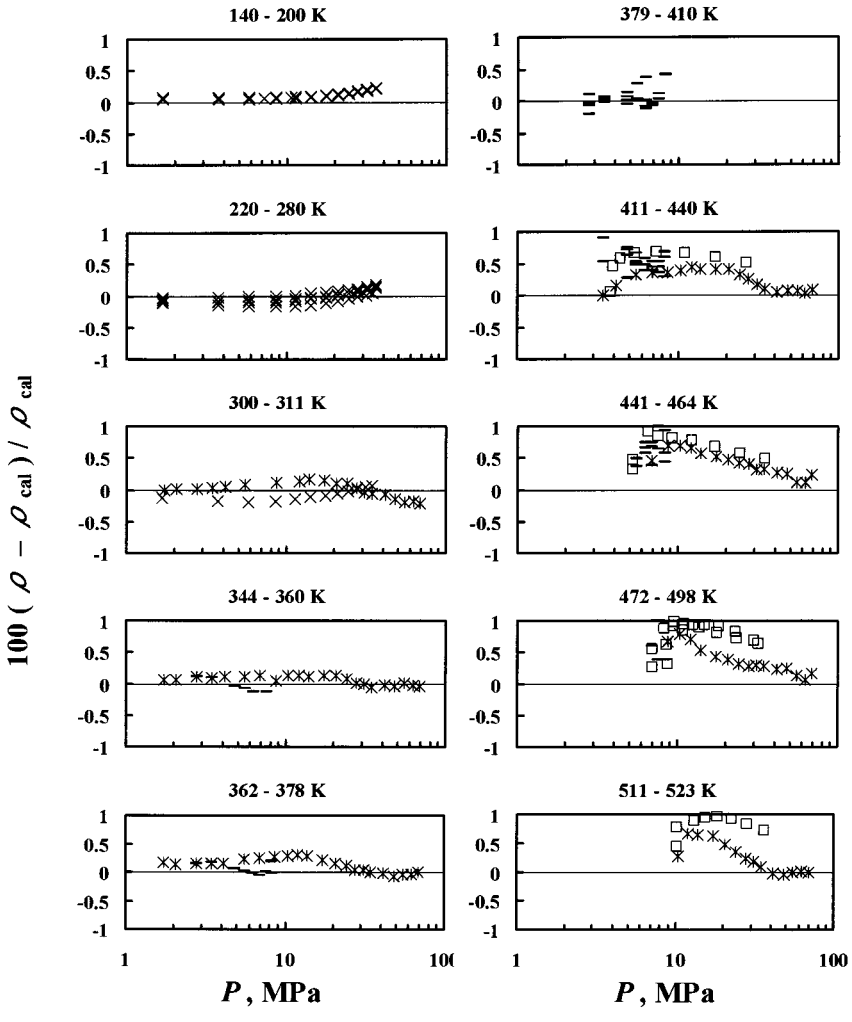

Fig. 4. Density deviations of $P\rho T$ property data from Eq. (4). (□) Beattie et al. [7]; (–) Kay [8]; (∗) Olds et al. [9]; (×) Haynes [10].

in Eqs. (1)–(3) are represented within ±1.0% in the range of validity of the present model except for the ρ'' values near the triple-point temperature, as clearly shown in Figs. 9 to 11. As a result, the present model represents the P_S measurements by Flebbe et al. [18] and Kratzke et al. [19] within ±0.09%, while the calculated P_S values at lower temperatures by Magee [29] agree with the present equation of state within ±0.82% (±0.2 kPa). As shown in Figs. 10 and 11, the ρ'' data of Olds et al. [9]

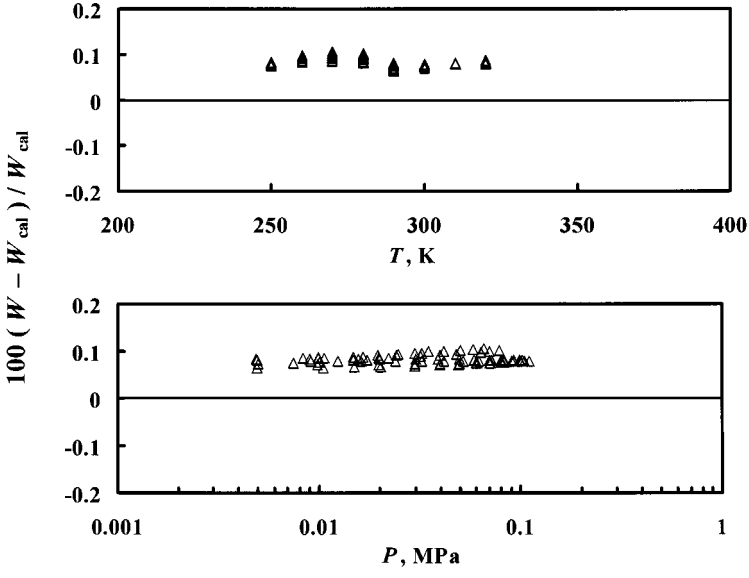

Fig. 5. Deviations of the speed-of-sound data in the vapor phase from Eq. (4). (△) [W] Ewing et al. [16].

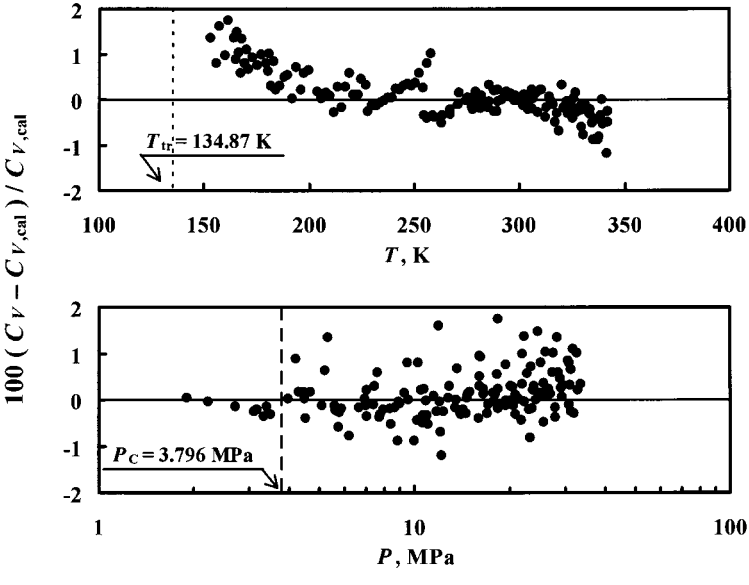

Fig. 6. Deviations of the isochoric heat capacity data in the liquid phase from Eq. (4). (●) [C_V] Magee and Lüddecke [12].

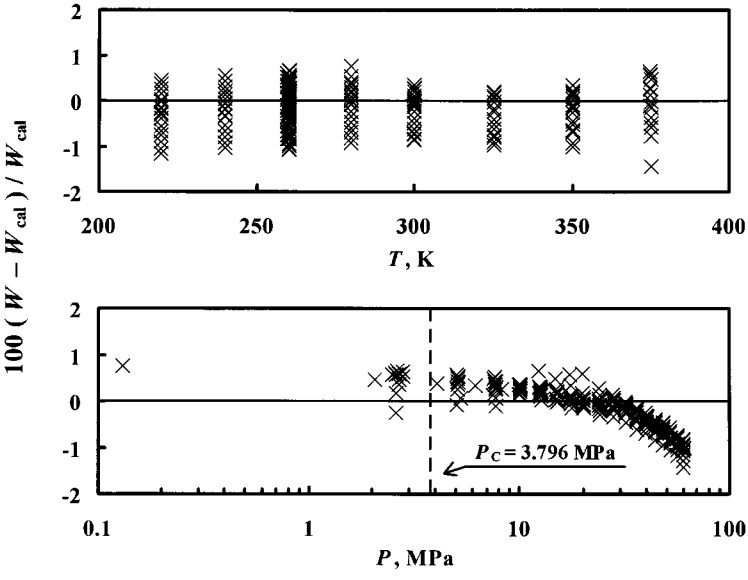

Fig. 7. Deviations of the speed-of-sound data in the liquid phase from Eq. (4). (×) [*W*] Niepmann [15].

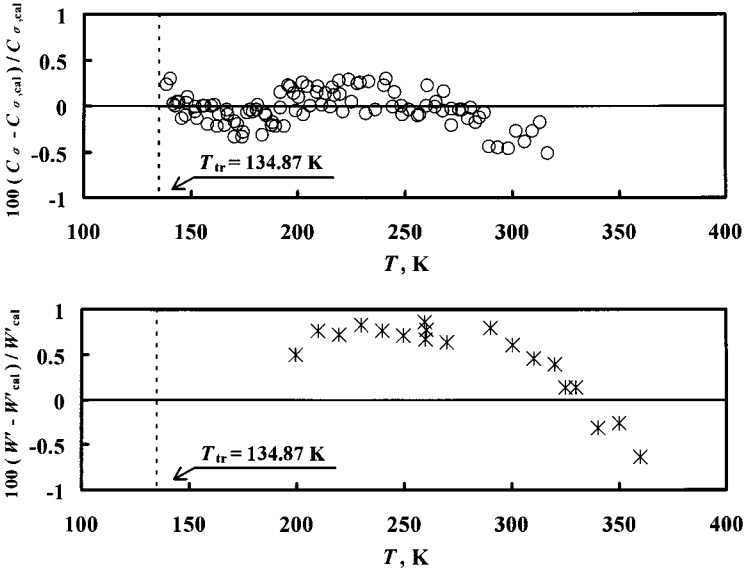

Fig. 8. Deviations of the saturated-liquid heat capacity and speed-of-sound data from Eq. (4). (○) [C_σ] Magee and Lüddecke [12]; (⁎) [*W′*] Niepmann [15].

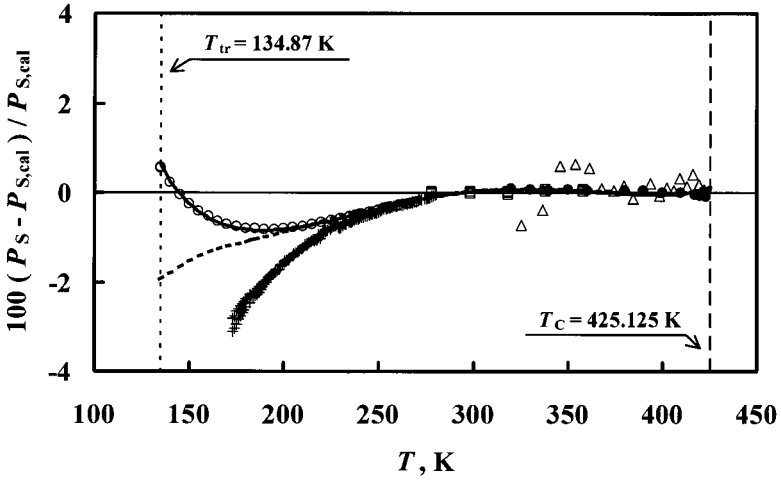

Fig. 9. Deviations of measured and calculated vapor pressure values from the present model. (△) Kay [8]; (□) Flebbe et al. [18]; (●) Kratzke et al. [19]; (+) Machin and Golding (additional two data points: +18.3%, −19.5%) [21]; (○) Magee [29]; (–) Eq. (1), (---) Younglove and Ely model [5].

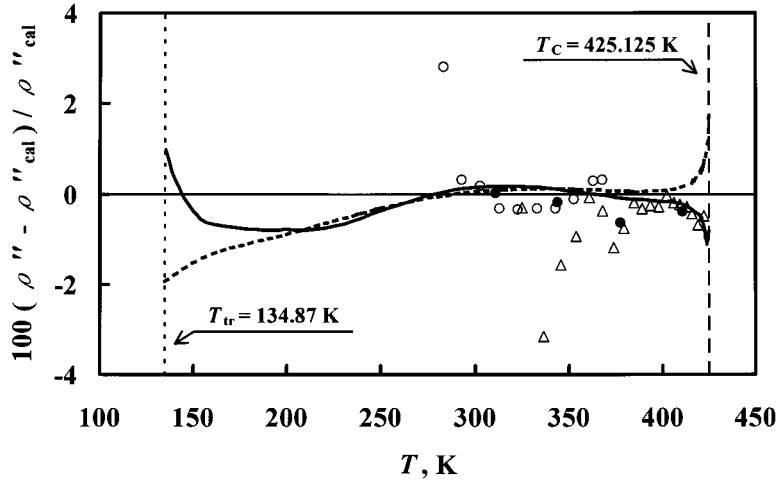

Fig. 10. Deviations of measured and calculated saturated-vapor densities ρ'' from the present model. (△) Kay [8]; (●) Olds et al. [9]; (○) Sliwinski [23]; (–) Eq. (2), (---) Younglove and Ely model [5].

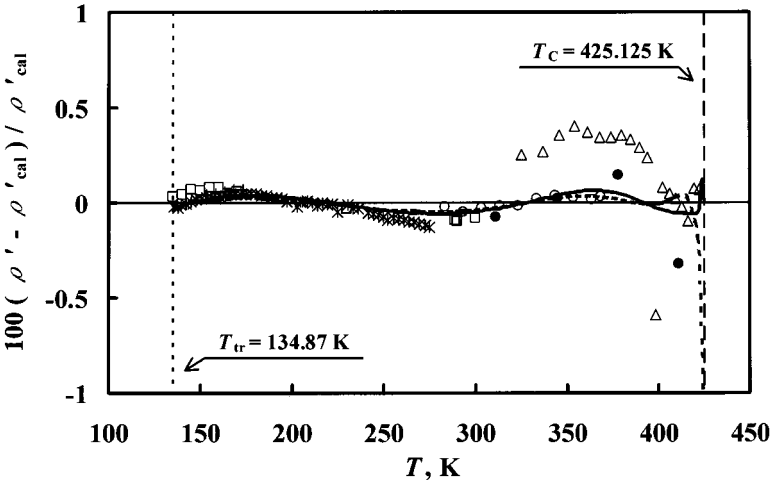

Fig. 11. Deviations of measured and calculated saturated-liquid densities ρ' from the present model. (△) Kay [8]; (●) Olds et al. [9]; (○) Sliwinski [23]; (+) McClune [24]; (□) Haynes and Hiza [25]; (∗) Orrit and Laupretre [26]; (–) Eq. (3), (- - -) Younglove and Ely model [5].

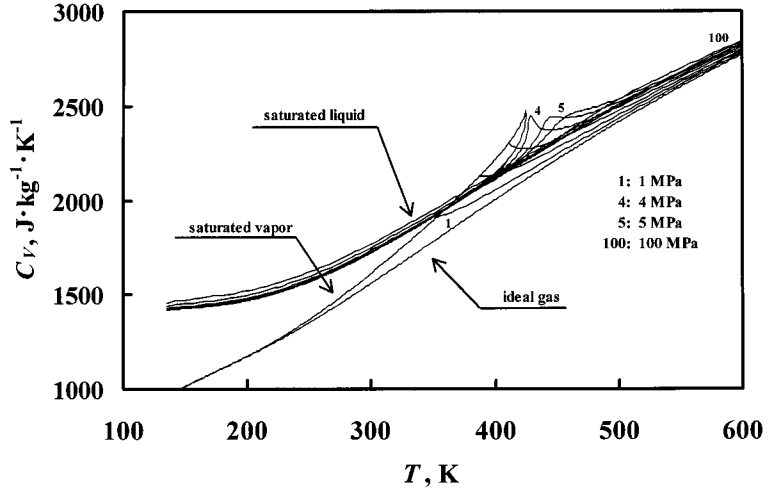

Fig. 12. Calculated isochoric heat capacity values along isobars using the present model.

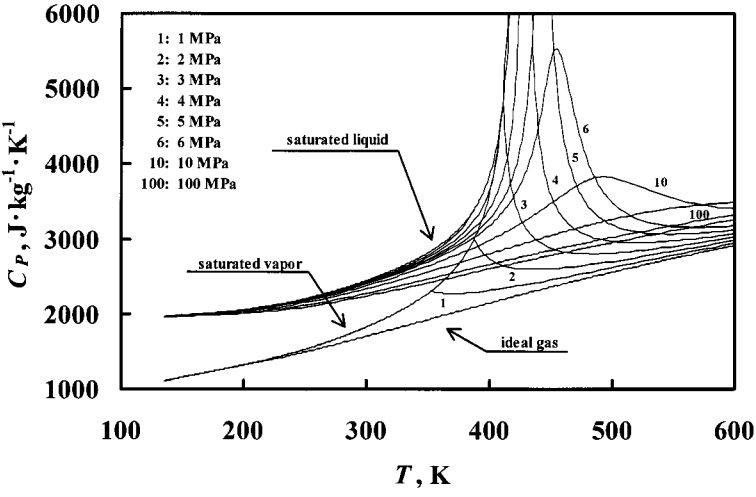

Fig. 13. Calculated isobaric heat capacity values along isobars using the present model.

and Sliwinski [23] are represented within $\pm 0.40\%$ except for a single datum of each series, while the ρ' data of Sliwinski [23], McClune [24], Haynes and Hiza [25], and Orrit and Laupretre [26] are well represented within $\pm 0.13\%$. Significant deviations of the ρ'' and ρ' data of Kay [8] can also be observed in Figs. 10 and 11.

As one of the most important tests for the accuracy of a thermodynamic property model, the behaviors of C_V and C_P over an extended range of temperature and pressure are shown in Figs. 12 and 13, respectively. From the physically reasonable behaviors shown in both figures over the entire range including the extrapolated region where no experimental data are available, it is confirmed that the present model does exhibit satisfactory thermodynamic consistency over the entire fluid phase of *n*-butane.

6. CONCLUSION

We have developed an equation of state for *n*-butane that is valid for temperatures from 134.87 K (the triple-point temperature) to 589 K, at pressures up to 69 MPa, and at densities up to 745 $kg \cdot m^{-3}$. The accurate experimental thermodynamic property data of *n*-butane are satisfactorily represented, and the smooth behaviors of the calculated isochoric and isobaric heat capacity values have also been confirmed in the range of validity of the present model.

ACKOWLEDGMENT

The authors are grateful to Dr. J. W. Magee, NIST, Boulder, who kindly provided his unpublished data, which were useful for our study.

REFERENCES

1. R. Tillner-Roth and A. Yokozeki, *J. Phys. Chem. Ref. Data* **26**:1273 (1997).
2. R. Tillner-Roth and H. D. Baehr, *J. Phys. Chem. Ref. Data* **23**:657 (1994).
3. E. W. Lemmon and R. T. Jacobsen, to appear in *J. Phys. Chem. Ref. Data* (2001).
4. H. Miyamoto and K. Watanabe, *Int. J. Thermophys.* **21**:1045 (2000).
5. B. A. Younglove and J. F. Ely, *J. Phys. Chem. Ref. Data* **16**:577 (1987).
6. M. O. McLinden, S. A. Klein, E. W. Lemmon, and A. P. Peskin, *NIST Thermodynamic and Transport Properties of Refrigerants and Refrigerant Mixtures (REFPROP), Version 6.01* (U.S. Department of Commerce, Washington, DC, 1998).
7. J. A. Beattie, G. L. Simard, and G.-J. Su, *J. Am. Chem. Soc.* **61**:26 (1939).
8. W. B. Kay, *Ind. Eng. Chem.* **32**:358 (1940).
9. R. H. Olds, H. H. Reamer, B. H. Sage, and W. N. Lacey, *Ind. Eng. Chem.* **36**:282 (1944).
10. W. M. Haynes, *J. Chem. Thermodyn.* **15**:801 (1983).
11. D. Gupta and P. T. Eubank, *J. Chem. Eng. Data* **42**:961 (1997).
12. J. W. Magee and T. O. D. Lüddecke, *Int. J. Thermophys.* **19**:129 (1998).
13. B. H. Sage, D. C. Webster, and W. N. Lacey, *Ind. Eng. Chem.* **29**:1309 (1937).
14. B. P. Dailey and W A. Felsing, *J. Am. Chem. Soc.* **65**:44 (1943).
15. R. Niepmann, *J. Chem. Thermodyn.* **16**:851 (1984).
16. M. B. Ewing, A. R. H. Goodwin, M. L. McGlashan, and J. P. M. Trusler, *J. Chem. Thermodyn.* **20**:243 (1988).
17. L. C. Kahre, *J. Chem. Eng. Data* **18**:267 (1973).
18. J. L. Flebbe, D. A. Barclay, and D. B. Manley, *J. Chem. Eng. Data* **27**:405 (1982).
19. H. Kratzke, E. Spillner, and S. Müller, *J. Chem. Thermodyn.* **14**:1175 (1982).
20. H. Holldorff and H. Knapp, *Fluid Phase Equil.* **40**:113 (1988).
21. W. D. Machin and P. D. Golding, *J. Chem. Soc. Faraday. Trans.* **85**:2229 (1989).
22. T. Sako, S. Horiguchi, H. Ichimaru, and S. Nakagawa, *J. Chem. Eng. Data* **42**:169 (1997).
23. P. Sliwinski, *Z. Phys. Chem. Neue Folge* **63**:263 (1969).
24. C. R. McClune, *Cryogenics* **16**:289 (1976).
25. W. M. Haynes and M. J. Hiza, *J. Chem. Thermodyn.* **9**:179 (1977).
26. J. E. Orrit and J. M. Laupretre, *Adv. Cryogen. Eng.* **23**:573 (1978).
27. J. G. Aston and G. H. Messerly, *J. Am. Chem. Soc.* **62**:1917 (1940).
28. W. M. Haynes and R. D. Goodwin, NBS Monograph 169 (U.S. Department Commerce, Washington, DC, 1982), p.197.
29. J. W. Magee, personal communication (National Institute of Standards and Technology, Boulder, CO, 1999).
30. P. J. Mohr and B. N. Taylor, *J. Phys. Chem. Ref. Data* **28**:1713 (1999).
31. T. B. Coplen, *J. Phys. Chem. Ref. Data* **26**:1239 (1997).
32. S. S. Chen, R. C. Wilhoit, and B. J. Zwolinski, *J. Phys. Chem. Ref. Data* **4**:859 (1975).
33. R. Tillner-Roth, personal communication (University of Hannover, Hannover, Germany, 1996).
34. W. Wagner, *Fortschr.-Ber. VDI-Z*, Reihe 3, No. 39 (1974).